Geoderma 165 (2011) 1–11

Contents lists available at ScienceDirect

Geoderma

journal homepage: www.elsevier.com/locate/geoderma

A simplified approach for estimating soil carbon and nitrogen stocks in semi-arid complex terrain

Melvin L. Kunkel *, Alejandro N. Flores, Toni J. Smith, James P. McNamara, Shawn G. Benner

Boise State University, Boise, Idaho, USA

ARTICLE INFO

Article history:
Received 31 July 2010
Received in revised form 5 March 2011
Accepted 21 June 2011
Available online 20 July 2011

Keywords:
Soil carbon
Insolation
NDVI
Statistical model
Semi-arid

ABSTRACT

We investigated soil carbon (C) and nitrogen (N) distribution and developed a model, using readily available geospatial data, to predict that distribution across a mountainous, semi-arid, watershed in southwestern Idaho (USA). Soil core samples were collected and analyzed from 133 locations at 6 depths ($n=798$), revealing that aspect dramatically influences the distribution of C and N, with north-facing slopes exhibiting up to 5 times more C and N than adjacent south-facing aspects. These differences are superimposed upon an elevation (precipitation) gradient, with soil C and N contents increasing by nearly a factor of 10 from the bottom (1100 m elevation) to the top (1900 m elevation) of the watershed. Among the variables evaluated, vegetation cover, as represented by a Normalized Difference Vegetation Index (NDVI), is the strongest, positively correlated, predictor of C; potential insolation (incoming solar radiation) is a strong, negatively correlated, secondary predictor. Approximately 62% (as R^2) of the variance in the C data is explained using NDVI and potential insolation, compared with an R^2 of 0.54 for a model using NDVI alone. Soil N is similarly correlated to NDVI and insolation. We hypothesize that the correlations between soil C and N and slope, aspect and elevation reflect, in part, the inhibiting influence of insolation on semi-arid ecosystem productivity via water limitation. Based on these identified relationships, two modeling techniques (multiple linear regression and cokriging) were applied to predict the spatial distribution of soil C and N across the watershed. Both methods produce similar distributions, successfully capturing observed trends with aspect and elevation. This easily applied approach may be applicable to other semi-arid systems at larger scales.

1. Introduction

Large spatial variation in soil carbon (C) content in topographically and ecologically diverse landscapes make quantification difficult (Arrouays et al., 1998; Garcia-Pausas et al., 2007; Jobbagy and Jackson, 2000; Kulmatiski et al., 2004; Yimer, 2007). Given the importance of the soil reservoir as a potential source or sink of atmospheric CO_2, there is a need for easily applied tools to improve estimates of soil C inventories (Foley and Ramankutty, 2004). The development of such tools can also elucidate underlying influences on the amount and spatial distribution of C in the soil reservoir.

In complex terrain, large variations in soil C are often observed with changing elevation, slope, aspect and hillslope position. These physical characteristics have been used to predict soil C distribution (e.g. Garcia-Pausas et al., 2007; Tsui et al., 2004). Other physical characteristics used to predict C distribution include soil depth, texture, and bulk density (e.g. Arrouays et al., 2006; Don et al., 2007; Garcia-Pausas et al., 2007). Because aboveground biological activity is the primary source of soil C, a strong positive correlation is often found between net primary productivity and soil C content (Carrera et al., 2009; Hooker et al., 2008; Jobbagy and Jackson, 2000). Remotely sensed vegetation parameters can be used as surrogates for ecological productivity (Curran et al., 1992; Scanlon et al., 2002) and these data have been successfully used to predict below ground C stocks (Burnham and Sletten, 2010; Paruelo et al., 2010). Many of these relationships have been exploited to predictively map the distribution of soil C using both statistical and geostatistical approaches (Arrouays et al., 1998; Camarero et al., 2009; Delbari et al., 2010; Vasques et al., 2010).

In most ecosystems, ecological productivity positively correlates to incoming solar radiation (insolation). In these systems, higher insolation produces higher ecological productivity (Dingman and Koutz, 1974; Lee, 1964). This relationship is often incorporated into the biogeochemical models of net primary productivity and associated soil C content (Law et al., 2001; Melillo et al., 1995). However, in arid and semi-arid environments, where the ecosystems are water limited, higher insolation can increase water stress and limit ecological activity (Rodriguez-Iturbe et al., 2001; Yetemen et al., 2010). In such ecosystems, ecological productivity can be inversely related to potential insolation (Beaudette and O'Geen, 2009; Reid, 1973; Wang et al., 2009). It is, therefore, probable that in semiarid ecosystems the distribution of soil C stocks will follow these

* Corresponding author at: Department of Geosciences, Boise State University, 1910 University Drive, Boise, Idaho, 83725-1535, USA. Tel.: +1 208 426 1631; fax: +1 208 426 4061.
E-mail address: melkunkel@u.boisestate.edu (M.L. Kunkel).

0016-7061/$ – see front matter © 2011 Elsevier B.V. All rights reserved.
doi:10.1016/j.geoderma.2011.06.011

vegetation trends that are modulated through feedbacks between insolation and soil moisture.

We hypothesize that distribution of soil C in semi-arid systems will, for a given vegetation density, be inversely related to the magnitude of insolation and we propose this easily retrieved variable can be used to improve prediction of soil C in complex terrain. The objectives of this study were to: 1) quantify the spatial distribution of soil carbon in a topographically complex, semi-arid, watershed, 2) evaluate the degree to which readily available landscape metrics, inclusive of insolation, can be used to describe soil C occurrence, and 3) use these variables to develop models to predict soil C distributions across the landscape.

2. Material and methods

2.1. Study sites and land use history

Dry Creek Experimental Watershed (DCEW) is located in the semi-arid southwestern region of Idaho, approximately 16 km northeast of the city of Boise, Idaho USA (Figure 1). The ~28-km^2 watershed is primarily northeastward trending from a lower elevation of 1000 m (all elevations listed as 'above mean sea level') to 2100 m at the summit of the watershed. Three meteorological stations located in the DCEW provide continuous monitoring of air temperature, precipitation, wind speed and direction, and radiation (DCEW, 2010). These weather stations range in elevations from 1146 m to 1850 m. Another meteorological station providing similar information is located at an elevation of 1932 m just north of the DCEW boundary at the Bogus Basin SNOTEL Site, operated by the U.S. Department of Agriculture's Natural Resources Conservation Service (NRCS, 2010). The dominant bedrock unit in the DCEW is biotite granodiorite (Lewis et al., 1987). In the lower elevations of the watershed, bedrock is overlain by Terteling Springs Formation sandstone (Burnham and Woods, 1992). Local soils are derived primarily from weathering of the Idaho Batholith and are divided into three general soil taxonomies – Argixerolls, Haploxerolls, and Haplocambids (Harkness, 1997). The depth and development of soils in DCEW correlates to the topographic and land cover attributes of DCEW with thicker soils found on northern aspects (Tesfa et al., 2009). Soils in DCEW are generally course-textured and well drained (Gribb et al., 2009; Harkness, 1997; Tesfa et al., 2009; Williams, 2005). Soils on northern aspects and at higher elevations have greater water storage capacity (Geroy et al., submitted for publication; Smith et al., submitted for publication) and provide a longer period of wet conditions into the growing season (Smith et al., submitted for publication); a likely contributor to the observed higher vegetation density on these slopes. At lower elevations, grass and sagebrush dominate both north and south aspects (DCEW, 2010). At middle elevations, southern facing aspects are characterized by grass and sagebrush with the northern facing aspects ranging from grass and deciduous shrubs to open forest communities of Ponderosa Pine and Douglas Fir (DCEW, 2010). At higher elevations, both north and south aspects are predominantly vegetated with Ponderosa Pine and Douglas Fir (DCEW, 2010). Portions of the upper elevations were logged in the mid 1970s and those areas are transitioning from deciduous shrubs to immature conifer forests, as evidenced by areas of sparse tree density in aerial photographs (outlined in Figure 1).

2.2. Sample collection and laboratory analysis methods

Soil cores were collected at 133 locations using an elevation-nested sampling approach from 1120 to 1850 m across the watershed (Figure 1). Within each elevation increment, a series of samples was

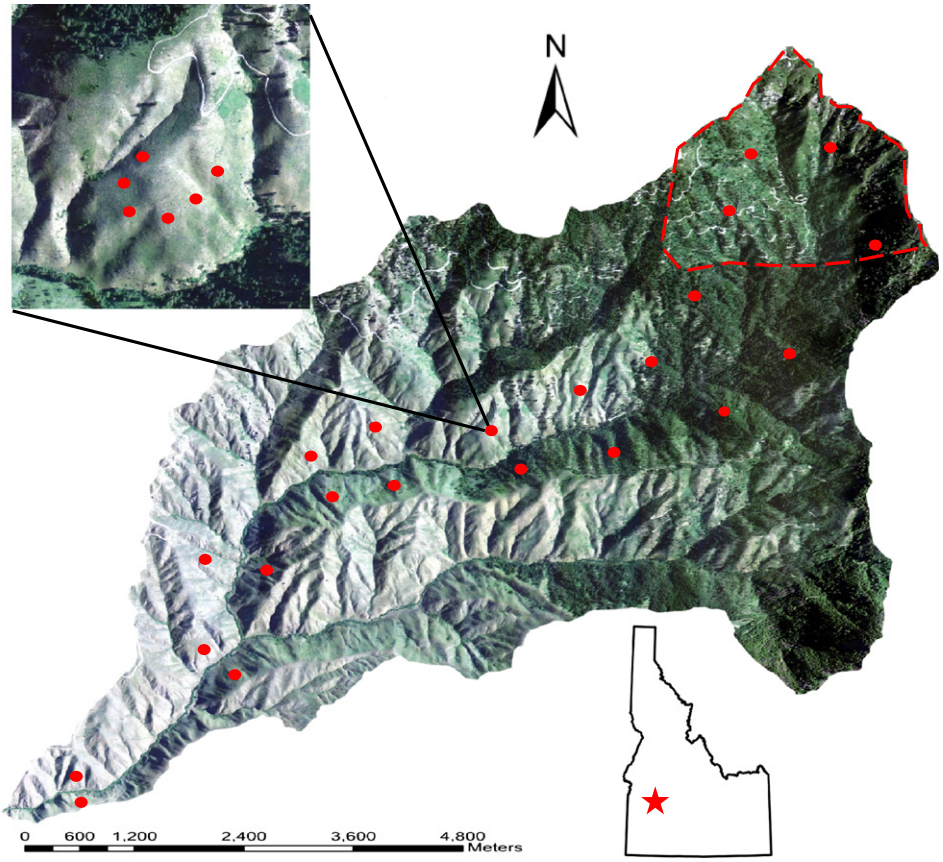

Fig. 1. Dry Creek Experimental Watershed, 16 km NE of Boise Idaho, USA. General site locations are represented by solid red circles within the watershed. An example of core locations within a general site is shown in the subset photo (upper left). Area of past disturbance (logging) outlined with a dashed red line in the upper watershed.

collected on opposing north and south-facing slopes. On each slope, six soil cores were sampled along an elevation contour (at 20–30 m spacing) to capture local variation in aspect. An additional soil core was taken in the upper elevation to capture an elevation/aspect combination not well represented in the primary sampling. Mid-slope locations were selected for sampling because previous work suggested that they are representative of average carbon (C) and nitrogen (N) values in a watershed (Franzmeier et al., 1969; Norton et al., 2004; Rhoton et al., 2006). Furthermore, in DCEW mid-slope C and N values are generally representative of hillslope-average values of C and N (Geroy, 2010).

At each sampling site, a 5 cm diameter, 30 cm deep core, sectioned into six 5 cm increments, was collected and stored at −5 °C in sealed bags until laboratory analysis. This approach yielded 798 samples. Field triplicates were collected at eight sites. All samples were dried in an oven at 105 °C and then sieved to 2 mm. Soil fractions less than 2 mm were homogenized, sub-sampled and then powdered to less than 250 μm in preparation for analysis.

Total C and N concentrations were determined by dry combustion using a Thermo Flash EA 1112 Elemental Analyzer following section 4H2a1 of the Natural Resources Conservation Service (NRCS) Soil Survey Laboratory Methods Manual (2004). Analysis standardization was based upon aspartic acid standards; this material was analyzed as an internal standard. Laboratory replicates, both between runs and during runs quantified instrument drift. Instrument drift averaged 1.1% for C with aspartic acid, while lab duplicates of soil samples varied by an average of 3.1% for C and field duplicates (generally collected within one meter of one another) varied by an average of 7.8% for C. Similarly, average instrument drift with aspartic acid, variation between lab duplicates, and variation for field duplicates was 3.6%, 6.9%, and 12.5%, respectively, for N. Organic/inorganic fractionation was performed by pre-treating 80 representative samples with 2–3 drops of concentrated HCl or H_3PO_4 (NRCS, 2004), samples were allowed to air dry in a fume hood until effervescence ceased. After effervescence, organic C fraction was determined using the Thermo Flash EA 1112 Elemental Analyzer. Inorganic C content was then calculated as the difference between total C and the organic C. Inorganic C fraction was <1% of the total C detected in all analyzed samples. Based upon the fractionation analysis, the total C is considered equivalent to total organic C for all samples. C and N by weight, and stocks were calculated using Eq. (1) (Batjes, 1996):

$$T_d = \sum_{i=1}^{k} \rho_i P_i D_i (1 - S_i) \quad (1)$$

where T_d is the total amount of C and N [Mg m^{-2}] over depth, d, ρ_i is the bulk density (Mg m^{-3}) of layer, i, P_i is the proportion of C and N [g C (N) g^{-1}] in layer i, D_i is the ith layer thickness (m), S_i is the volume of the fraction of fragments larger than 2 mm in layer i. To calculate C and N stocks, we used bulk density and particle size distribution values for the DCEW area published by the NRCS in its Soil Survey Geographic (SSURGO) dataset. Bulk densities and particle size distributions obtained from SSURGO compared favorably with quantities previously measured in DCEW (Smith, 2010; Geroy, 2010). C and N concentrations in each core were linearly aggregated to a depth of 30 cm and for comparison purposes converted to units of g C m^{-2} or g N m^{-2}.

2.3. Predictor variables

2.3.1. Elevation and precipitation

Precipitation was considered as a predictor variable because it is the source of moisture for ecosystem productivity. The spatial distribution of mean annual precipitation in DCEW was determined by first establishing an elevation-based precipitation lapse rate for the watershed based on the 10-year average precipitation for the three weather stations in DCEW and the Bogus Basin SNOTEL site. Mean annual precipitation increases from 37 cm at the bottom of DCEW to 89 cm at the top of the watershed. Both a linear model and a non-linear fit (Naoum and Tsanis, 2004; Ranhao et al., 2004) were performed and tested. The non-linear model produced a root mean square error in estimation of mean annual precipitation of 16.2 mm, compared with 34.3 mm for the linear model. The lapse rate model was then used with a hyposometric (area-elevation) function based on elevations from a 10 m digital elevation model (DEM) obtained from the United States Geological Survey (USGS) to predict mean annual precipitation throughout the watershed.

2.3.2. Potential insolation

Potential insolation (incoming solar radiation) depends on aspect, slope gradient, and elevation, which can be estimated directly from DEMs making it attractive as a predictor variable. Total annual potential insolation was calculated for the DCEW area using the Solar Radiation tool in ESRI ® ArcMap 10.0 based on the USGS 10 m DEM. Potential insolation only changes on the scales of obliquity (Loutre et al., 2004), eliminating the need to calculate a long-term average for the area. Calculated insolation values compared favorably to annual values of measured solar insolation at two weather stations (shortwave) in DCEW, as well as the SNOTEL Bogus Basin station (total), reflecting the fact that this environment is relatively cloud-free during the summertime peak-insolation period. Annual potential insolation for the entire DCEW ranges from 1700 kWatt m^{-2} to 460 kWatt m^{-2}, averaging 1300 kWatt m^{-2} (Table 1).

2.3.3. NDVI/vegetation

Total standing biomass or vegetative cover reflects total ecosystem productivity and is often proportional to the C and N input to the soil.

Table 1
Statistical results for all collected data in study.

	Mean	Median	Std dev	Maximum	Minimum	W	Pr<W*
Carbon (g m^{-2})	2100	1800	1200	6100	430	0.9034	<0.0001
Nitrogen (g m^{-2})	190	170	100	630	60	0.8662	<0.0001
Ratio (C:N)	10.1	10.3	2.2	16.4	6.2	0.9723	0.0082
NDVI	0.49	0.47	0.13	0.74	0.27	0.9288	<0.0001
Insolation (10^3 kWatt m^{-2})	1.26	1.34	0.24	1.61	0.75	0.9127	<0.0001
Precip (mm)	560	510	140	850	370	0.9135	<0.0001
Elevation (m)	1500	1400	230	1900	1100	0.9423	<0.0001
ASPECT (degrees)	200	190	100	360	0	0.9639	0.0013
Slope (%)	30	30	7	50	10	0.9836	0.1104

* Pr<W indicates the probability the data is normally distributed. If less than .05, the null hypothesis (of normality) is typically rejected.
1. Carbon, nitrogen and ratio data from collected/analyzed data.
2. NDVI calculated from Landsat 5 data (2008).
3. Insolation (potential) and elevation derived from USGS 10 m DEM.
4. Precipitation calculated from USGS 10 m DEM, using observed relationships within DCEW.
5. Aspect and slope values collected during field sampling.

The Normalized Difference Vegetation Index (NDVI) is a commonly used, and easily calculated, satellite image-based proxy for vegetative cover (Jensen, 2000; Jordan, 1969; Kriegler et al., 1969; Rouse et al., 1974). All available Landsat-5 Thematic Mapper imagery (that covered the watershed) at 30 m spatial resolution (http://edcsns17.cr.usgs.gov/EarthExplorer/) was collected for calendar year 2008. This year was considered average with respect to air temperature, precipitation, and NDVI in DCEW (DCEW, 2010; Smith, 2010). Temporal resolution of images is generally 16 days during cloud-free conditions. NDVI values were calculated in the ENVI software environment for each image on a

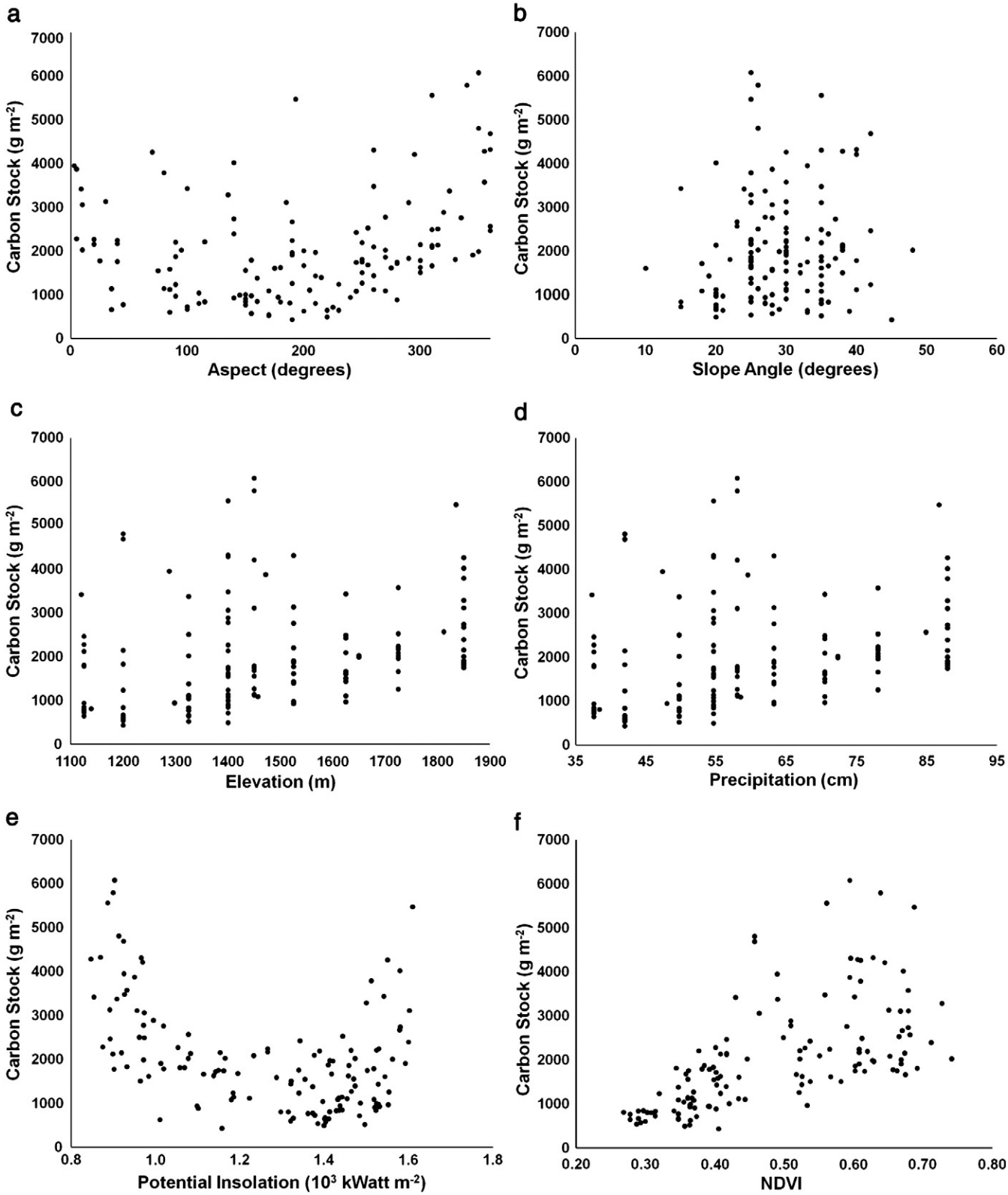

Fig. 2. Predictor variables plotted against carbon (C) stocks. a) Aspect vs C, b) Slope angle vs C, c) Elevation vs C, d) Precipitation vs C, e) Annual Potential Insolation [10^3 kWatt m^{-2}] vs C, f) NDVI vs C.

pixel-basis using the following previously developed formula (Jensen, 2000; Jordan, 1969; Kriegler et al., 1969; Rouse et al., 1974):

$$NDVI = \frac{(NIR - red)}{(NIR + red)} \quad (2)$$

where *NIR* is the reflectance signal in the near-infrared radiometric band and *red* is reflectance in the red band.

Mean monthly NDVI values were obtained for each Landsat pixel within the DCEW. A corresponding raster representing the peak NDVI for 2008 was obtained by selecting the maximum monthly NDVI value within each pixel. This annual maximum monthly mean value was used in the statistical analysis and modeling for C and N. The maximum monthly average NDVI for DCEW ranged from 0.16 to 0.80 with an average of 0.49. NDVI values from pixels containing the field data collection sites largely reflect the larger scale variability in annual maximum monthly mean NDVI, ranging from 0.27 to 0.74 with an average of 0.49 (Table 1). Annual maximum NDVI follows an approximately log normal distribution throughout the watershed (Table 1), being generally lower at lower elevations and on southern aspects and higher at upper elevations and on northern aspects.

2.4. Statistical analysis and modeling

Statistical analysis and modeling was conducted using SAS 9.1. Descriptive statistics were computed to examine relationships between total C and N and potential predictor variables aspect, slope, elevation, precipitation, NDVI, and insolation (Table 1, Figure 2). Similar correlations were observed between predictor variables and N (data not shown). A Shapiro–Wilk (W) test for normality showed all the spatially distributed data to be positively skewed with a best fit to a lognormal distribution. We therefore log transformed this data to reduce the skew, and subsequently standardized each predictor and response variable by subtracting the sample mean and dividing by the sample standard deviation, so that each variable was zero mean and unit variance. Standardization was performed to compensate for the between-variable disparity in the magnitudes of untransformed predictor and response variables. This allowed assessment of the relative importance of individual predictor variables in the developed multivariate statistical models. Predicted values of C and N represent standardized quantities. Therefore, for the developed predictive models to be broadly applicable some estimate of the regional mean and variance in soil C and N must be known or estimated. For this preliminary investigation into drivers of hillslope-scale variation in C and N and their relative importance in this semi-arid montane environment, however, the use of standardized quantities is appropriate because statistical models using the non-standardized data produced similar degrees of correlation.

Least squares regression analysis was used to develop predictive models of C and N stocks, as well as assess the robustness of developed models to reproduce observed C and N excluded from model development through a k-fold cross-validation. This model development and cross-validation procedure were performed for each predictor variable individually and for every combination of predictor variables. As expected, given the direct co-dependence, calculated precipitation showed no improvement over elevation to predict C and N, and was excluded in further model building. Tables 3 and 4 show developed regression models performance in predicting observed C and N. Insolation and NDVI were the most powerful predictors of soil C and N.

Utilizing these identified predictor relationships, models to predict the spatial distribution of soil C and N across the watershed were developed using both multiple linear regression and cokriging analysis. In the multiple linear regression model approach, developed equations, coupled with spatially distributed NDVI and potential insolation data, were used to predict the soil C and N content at each 10×10 m pixel in the modeling domain. In the second set of models, a simple cokriging analysis was performed (ESRI ® ArcMap 10.0 Geostatistical Analyst toolbox) to develop a predictive maps of soil C and N and estimation errors using insolation and NDVI as covariates. Simple cokriging is a widely used method of spatially interpolating a sparsely sampled variable (in this case C or N) to finer resolutions by using spatial information from more intensely measured quantities that are covariates of the predictand (in this case insolation and NDVI) (Webster and Oliver, 2007). Cokriging is a multivariate extension of kriging and relies on a linear model of co-regionalization that exploits not only the autocorrelation in the primary variable, but also the cross-correlation between the primary variable and secondary variables; because of these qualities, we expected that cokriging would represent the observed trends equally well if not better than the regression models.

Because mid-slope C and N values may be different from those located away from mid slope positions, we calculated the Topographic Position Index (TPI) for each 10 m DEM pixel using ESRI ® ArcMap 10.0 with the Land Facet Corridor Tools developed by CorridorDesigns (Majka et al., 2007). We combined the TPI with the slope position C and N relationships identified by Geroy (2010) to develop a slope adjustment index for the DCEW. This index was then applied to model output, similar to the approaches used by Florinsky et al. (2002) and Webster et al. (2011). As a final step, the standardized model values were then converted back to non-standardized values of C and N using the observed mean and standard deviation. Therefore, the values reported in all tables and figures are stock values (g C or N m^{-2}).

3. Results

3.1. General trends in spatial distribution of C and N

The average total carbon (C) and nitrogen (N) stock of the upper 30 cm of soil in the study area was 2100 (g m^{-2}) and 190 (g m^{-2}), respectively, with an average C:N ratio of 10.1 (Table 1), these observations are consistent with other semi-arid regions of the world (McClaran et al., 2008; Shrestha and Stahl, 2008). The C content increases with elevation and is higher on northern aspects. The average C content at lower elevations and on south-facing aspects is 930 g C m^{-2}, vs an average of 2600 g C m^{-2} for north facing aspects at higher elevations (Table 2). At forested higher elevations, where vegetation distribution is more uniform, the difference in soil C with aspect is less pronounced. In general, these results agree with those from similar climatic regimes (Thompson and Kolka, 2005, Zhusi, 2006). As is commonly observed, C and N stocks decline with depth (Figure 3). Trends in soil N closely follow trends in C. Further discussion will be limited to the spatial distribution of C, except where significant differences between C and N trends occur. Smaller C:N ratios are observed at the lower elevations and on southern aspects and C:N ratios also decline with depth (Figure 3).

Table 2
Contrasting differences in carbon and nitrogen by aspect and elevation. Units are g m^{-2}.

	Mean	Range	Std dev
Carbon			
Lower [a]	1700	430–5600	1200
Upper[b]	2300	930–6100	1100
Lower South Facing[a]	930	500–1800	340
Upper South Facing[b]	2100	930–4300	900
Lower North Facing[a]	2500	430–5600	1400
Upper North Facing[b]	2600	1100–6100	1300
Nitrogen			
Lower[a]	170	60–480	100
Upper[b]	210	100–630	90
Lower South Facing[a]	120	80–190	30
Upper South Facing[a]	190	100–350	70
Lower North Facing[a]	230	60–480	110
Upper North Facing[a]	220	120–630	110

[a] Lower elevation range: 1120–1450 m.
[b] Upper Elevation range: 1450–1850 m.

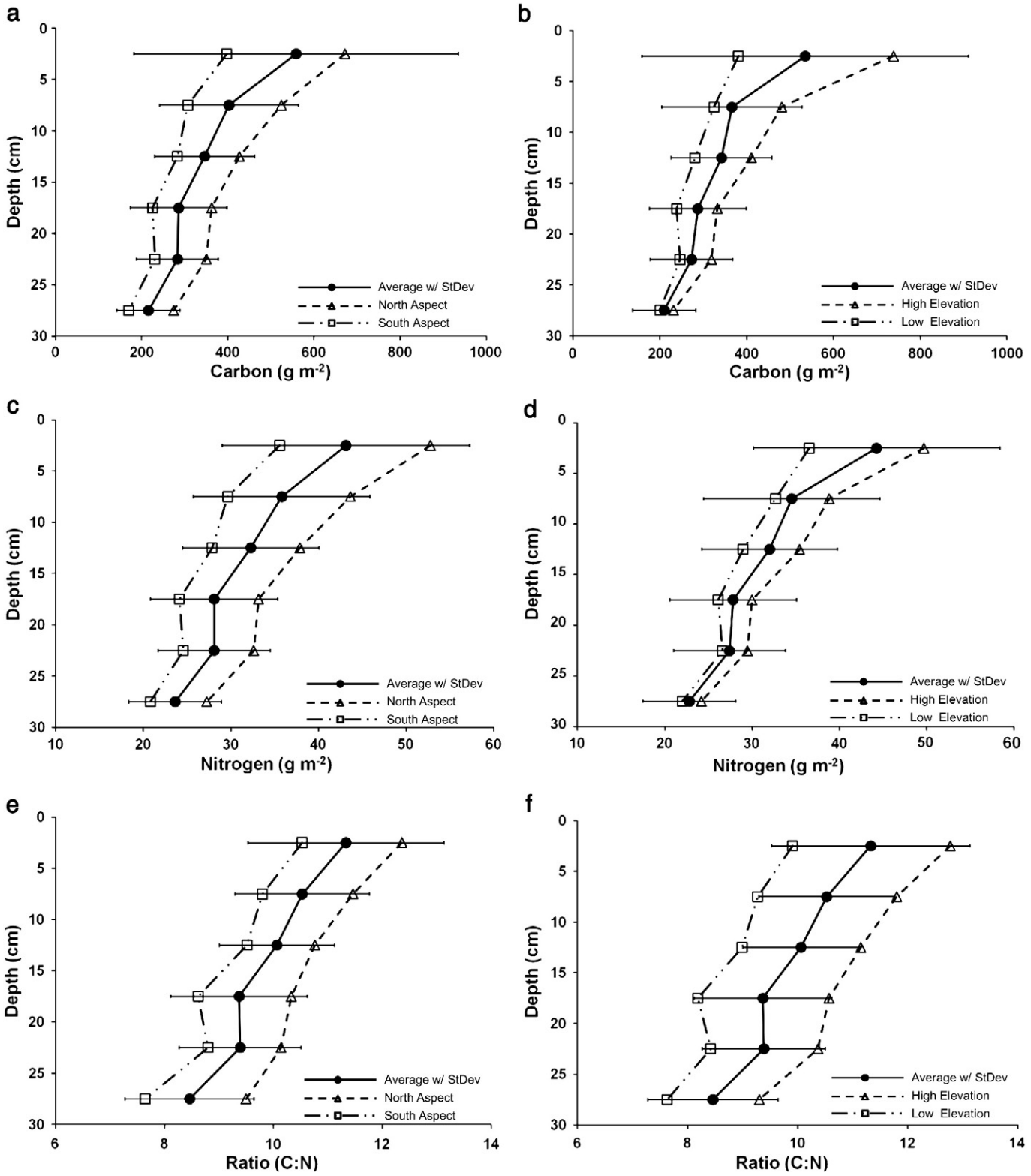

Fig. 3. Carbon (C), nitrogen (N) and C:N ratio depth profiles. a) C depth profile by aspect, b) C depth profile by elevation, c) N depth profile by aspect, d) N depth profile by elevation, e) ratio profile by aspect, f) ratio profile by elevation.

3.2. Predictors of soil C and N

Normalized Difference Vegetation Index (NDVI), potential insolation, elevation, aspect, and slope were identified as potential predictors of soil C distribution. Individually, aspect, slope, and elevation describe only a small amount of the variance in soil C stocks (Table 3). In contrast, potential insolation and NDVI each independently explain significantly more of the variance in soil C with notably larger R^2 values (Table 3). As expected, NDVI is positively correlated to soil C content, reflecting the commonly observed relationship between above and below-ground C reservoir sizes. Interestingly, potential insolation, exhibits a higher correlation than the combined variables of slope,

Table 3
Statistical results of linear regression models for predicting carbon distribution in DCEW.

Terms	Regression statistics
Aspect	$R^2 = 0.00$, $F(1,132) = 0.05$, $p = .8261$
Slope	$R^2 = 0.02$, $F(1,132) = 3.11$, $p = .0803$
Aspect, Slope	$R^2 = 0.03$, $F(2,131) = 1.64$, $p = .1948$
Elevation	$R^2 = 0.17$, $F(1,132) = 26.75$, $p < .0001$
Aspect, Elevation	$R^2 = 0.17$, $F(2,131) = 13.43$, $p < .0001$
Slope, Elevation	$R^2 = 0.21$, $F(2,131) = 17.01$, $p < .0001$
Slope, Elevation, Aspect	$R^2 = 0.21$, $F(3,130) = 11.59$, $p < .0001$
Insolation	$R^2 = 0.22$, $F(1,132) = 32.95$, $p < .0001$
NDVI	$R^2 = 0.54$, $F(1,132) = 152.10$, $p < .0001$
NDVI, Aspect, Slope, Elevation	$R^2 = 0.60$, $F(4,129) = 48.32$, $p < .0001$
NDVI, Insolation (all data)	$R^2 = 0.62$, $F(2,131) = 108.49$, $p < .0001$
NDVI, Insolation (final model[a])	$R^2 = 0.81$[b], $F(2,106) = 223.42$, $p < .0001$

[a] The final model (NDVI and Insolation), was built with data from the disturbed area (logged) removed.
[b] An R^2 of 0.78 was achieved when the final model was applied to all observed data (including disturbed area data which had been removed during modeling building).

aspect, and elevation. It is also noteworthy that potential insolation is inversely related to soil C content. It is recognized that there is likely some degree of colinearity between potential insolation and NDVI. The existence of this colinearity precludes quantitative evaluation of the relative influence of these two variables on any solution produced by multiple linear regression and compromises the uniqueness of fit; it does not diminish the value of the overall relationship.

By allowing interaction in the predictive model between both potential insolation and NDVI, we achieved significant improvement in model performance, with an R^2 of 0.62 for C and 0.46 for N, statistically significant at $p<0.0001$ (Tables 3 and 4). Eqs. (3) and (4) below represent the resulting multiple linear regression models for soil C and N as a function of NDVI and potential insolation:

$$C = 0.6665(NDVI) - 0.3040(I) \quad (3)$$

$$N = 0.45406(NDVI) - 0.3017(I) \quad (4)$$

where,

C	Normalized carbon stock ($g\ m^{-2}$),
N	Normalized nitrogen stock ($g\ m^{-2}$),
NDVI	Normalized maximum annual NDVI,
I	Normalized annual insolation.

Values of NDVI and potential insolation for each sample location are input to Eqs. (3) and (4) and the predicted values of C and N at those locations are compared with the respected observed quantities

Table 4
Statistical results of linear regression models for predicting nitrogen distribution in DCEW.

Terms	Regression statistics
Aspect	$R^2 = 0.00$, $F(1,132) = 0.00$, $p = .9732$
Slope	$R^2 = 0.01$, $F(1,132) = 1.38$, $p = .2430$
Aspect, Slope	$R^2 = 0.01$, $F(2,131) = 0.70$, $p = .4972$
Elevation	$R^2 = 0.09$, $F(1,132) = 13.06$, $p = .0004$
Aspect, Elevation	$R^2 = 0.09$, $F(2,131) = 6.51$, $p = .0020$
Slope, Elevation	$R^2 = 0.11$, $F(2,131) = 7.90$, $p = .0006$
Slope, Elevation, Aspect	$R^2 = 0.11$, $F(3,130) = 5.3$, $p = .0018$
Insolation	$R^2 = 0.17$, $F(1,132) = 27.89$, $p < .0001$
NDVI	$R^2 = 0.37$, $F(1,132) = 76.35$, $p < .0001$
NDVI, Aspect, Slope, Elevation	$R^2 = 0.45$, $F(4,129) = 25.91$, $p < .0001$
NDVI, Insolation (all data)	$R^2 = 0.46$, $F(2,131) = 54.31$, $p < .0001$
NDVI, Insolation (final model[a])	$R^2 = 0.66$[b], $F(2,106) = 103.08$, $p < .0001$

[a] The final model (NDVI and Insolation), was built with data from the disturbed area (logged) removed.
[b] An R^2 of 0.62 was achieved when the final model was applied to all observed data (including disturbed area data which had been removed during modeling building).

(Figure 4). When sites within the watershed recently disturbed by logging ($n = 25$, see Figure 1) were removed from the dataset and the regression model was rebuilt using the entire dataset, the resulting performance improved to R^2 equals 0.81 for C and R^2 equals 0.66 for N (Tables 3 and 4):

$$C = 0.6324(NDVI) - 0.3729(I) \quad (5)$$

$$N = 0.5118(NDVI) - 0.3694(I) \quad (6)$$

3.3. Modeled spatial distribution of C and N

The developed relationships between C and N and the predictor variables NDVI and insolation were used to model the spatial distribution of C and N across the watershed applying both linear regression and cokriging techniques. The two modeling approaches produced similar spatial distribution maps of C and N for the watershed (Figure 5) and these results are consistent with the empirically observed trends (Table 5). Both models exhibit strong differences in soil C with aspect; north-facing slopes typically exhibit 5 times the C of adjoining soils on south-facing aspects. Similarly, the two models produced generally higher C at higher elevations; increasing by nearly a factor of 10 times on south-facing slopes from the bottom to the top of the watershed. Modeled N follows similar trends.

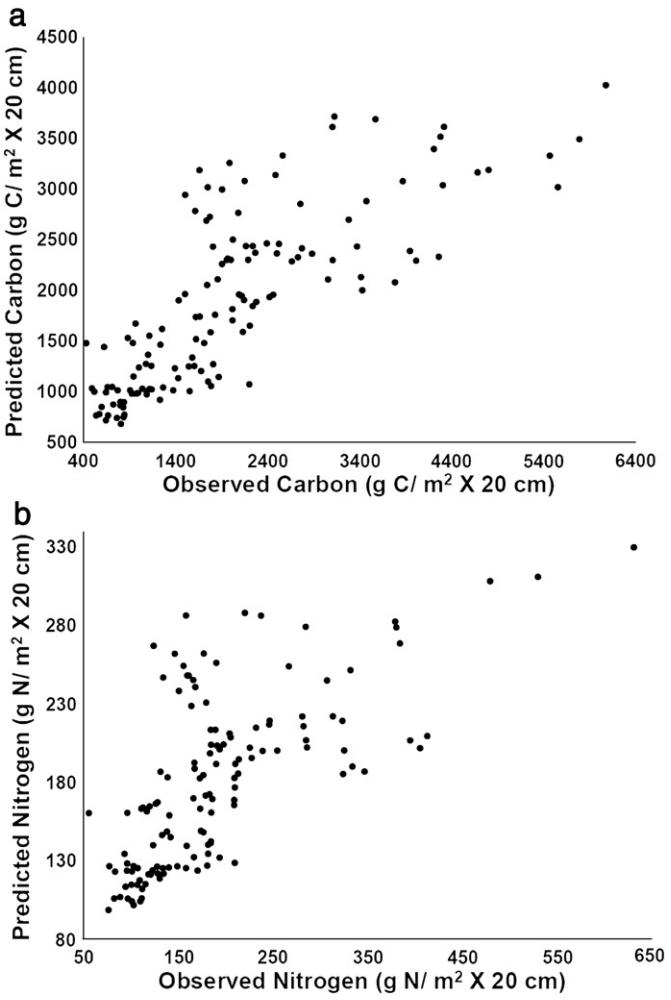

Fig. 4. a) Observed C stocks vs predicted C stocks using multiple linear regression with predictors of potential insolation and NDVI. b) Observed N stocks vs predicted N stocks using multiple linear regression with predictors of potential insolation and NDVI.

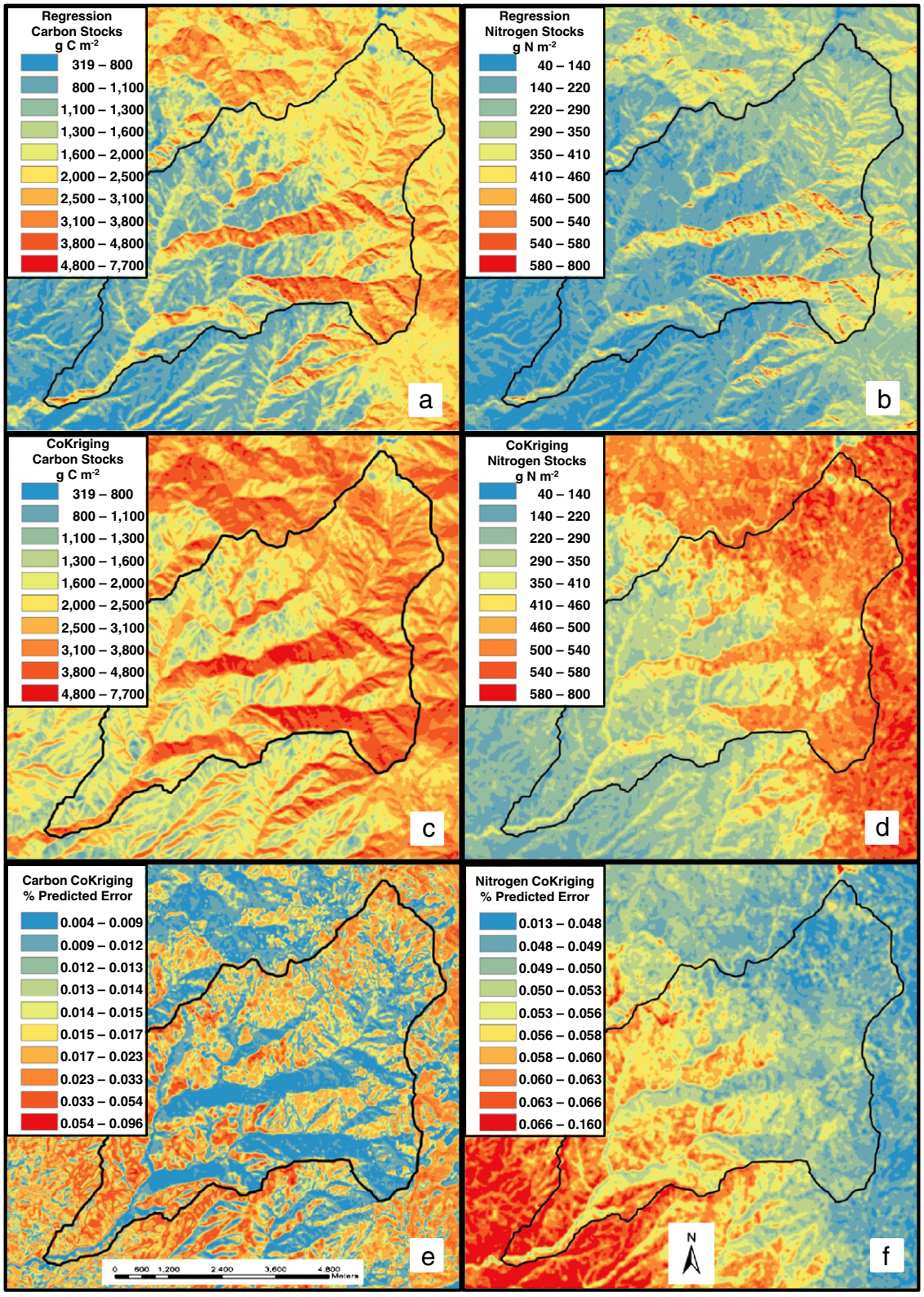

Fig. 5. a) Multiple Linear Regression modeled C stocks in DCEW and surrounding areas. b) Multiple Linear Regression modeled N stocks in DCEW and surrounding areas. c) Map resulting from ordinary co-kriging of potential insolation and NDVI to predict C stocks in DCEW and surrounding areas. d) Map of the predicted percent of error (prediction standard error divided by the predicted value) associated with the co-kriging of potential insolation and NDVI to predict C stocks in DCEW. e) Map resulting from ordinary co-kriging of potential insolation and NDVI to predict N stocks in DCEW and surrounding areas. f) Map of the predicted percent of error (prediction standard error divided by the predicted value) associated with the co-kriging of potential insolation and NDVI to predict N stocks in DCEW. All C and N stock values are for $m^2 \times 30$ cm. All data symbolized as a natural breaks (Jenks) classification with 10 classes using ESRI ® ArcMap 10.0.

Table 5
Observed and modeled soil carbon values (g C m^{-2}) values[a,b].

		Mean	Maximum	Minimum	Std dev
Observed		2100	6100	430	1200
Modeled	Regression	1800	7800	320	880
	Cokrigging	2600	6100	430	960

[a] Data for the upper 30 cm of soil depth.
[b] Observed are point values, regression and cokrigging are for entire modeled area and therefore are not expected to exhibit agreement.

While the overall trends in the two modeling approaches are similar, there are notable differences. Perhaps the most evident difference is generally higher C values in the cokrigged results compared to those produced by linear regression. The mean C content in the cokrigged results is 2600 g C m^{-2}, while the model-produced mean by regression is 1800 g C m^{-2}. The minimum and maximum values also vary between the model methods. In accordance with the cokriging approach, wherein modeled data are generated by interpolation, the maximum and minimum values are identical to the observed dataset. In contrast, the regression-generated maximum and minimum values reflect the ability of the method to produce values outside the range of that found in the observed dataset. Because observed data is composed of discrete point values, this dataset does not necessarily share a mean with that produced by model results and the degree of similarity in the mean values between observed and modeled values is not necessarily a reflection of model accuracy. Nevertheless, it is reassuring that both the regression and cokriging results produce mean values of similar magnitude to the observed data. The standard deviation for both analysis methods decreased appreciably from the observed 1200 (g C m^{-2}) to 880 for the regression and 960 for cokriging, reflecting the smoothing effect of both modeling approaches. Differences between modeling results for N follow those observed for C but are more pronounced. In particular, there is a strong deviation between model results for N values at high elevations; cokriging produces soil N contents that are nearly twice as high as those produced by the regression model.

A strength of the cokriging approach is that it produces a spatial distribution of percent error, computed as the ratio of the cokriging prediction standard error to the predicted value (Figure 5e and f). These error maps indicate that the error is not randomly distributed. In the case of both C and N, the error is generally highest where C is also high (higher elevation and north-facing slopes). Error in N estimates exhibits stronger elevation-based organization; error is higher at lower elevations compared to C.

4. Discussion

4.1. Underlying controls on soil carbon distribution

While not an explicit goal of this work, some discussion of the causal relationship between the identified predictors and soil carbon (C) and nitrogen (N) distribution is warranted. The correlation between soil C contents and vegetation density (as measured by NDVI) in the DCEW suggests that, as in many other ecosystems, soil C content is strongly dependent the rate of C input from aboveground vegetation. The observed negative correlation with insolation in this semi-arid landscape likely reflects the important and limiting role that soil moisture plays on vegetation growth and subsequently input of C to soil reservoirs. South-facing slopes receive more insolation and soils dry more quickly than north-facing slopes (Smith et al., submitted for publication). This likely contributes to higher vegetation densities on north-facing slopes where soil moisture limitation is reached later in the growing season. These aspect differences are overlain by a strong elevation gradient, which produces wetter and cooler conditions at higher elevations (Smith et al., submitted for publication). In the DCEW this precipitation gradient translates into a vegetation gradient in which more biomass is supported at higher elevations. This presumes that positive the influence of wetter conditions outweighs the potentially suppressive influence of lower temperatures on productivity. Again, soil C closely follows vegetation, exhibiting higher values at higher elevations. While often linked to insolation, temperature can exert a distinct, and often complex, influence on the soil C reservoir. For example, less insolation on north-facing slopes may reduce soil temperatures and inhibit soil respiration, resulting in a higher soil C content (Kane et al., 2005; Miller et al., 2004). Alternatively, lower temperatures can depress ecological productivity, producing declines in the soil C reservoir (Garcia-Pausas et al., 2007). In this system, we observe more soil C where temperatures are generally lower, a trend consistent with the former mechanism. These preliminary observations suggest a complex interaction among several biophysical and hydroclimatic processes, including the dynamics of soil moisture, insolation, and temperature. The ongoing study of these dynamics may better elucidate these relationships.

4.2. Importance of disturbance

As mentioned above, four of the sampling sites at tree-covered higher elevations (comprising 25 soil cores) were in areas deforested by logging in the 1970s (Figure 1). When we excluded the cores located in disturbed areas from regression modeling, we find a significant increase in the R^2 to 0.81 at $p<0.0001$ (Table 3). When we extrapolated the re-fit model to the 25 core sites in the logged areas, the model over-predicted C at each site by approximately 25%. A plausible interpretation of the regression model over-prediction is the previously documented time lag between vegetation regeneration and corresponding build-up of soil C stocks (Antos et al., 2003; Slesak et al., 2009; Vedrova et al., 2010; Yanai et al., 2003). Because NDVI is the most significant predictor of soil C, this over-prediction seems to suggest the association between NDVI and soil C is weaker at the disturbed sites vs undisturbed sites. This interpretation is based on the assumption that the relative rates of C cycling at undisturbed but forested sites at lower elevations approximately reflect the expected pre-disturbance relative rates of C cycling at the higher elevation forested sites. To confirm this explanation, future soil C sampling should be conducted in nearby undisturbed forests that exhibit vegetation and topographic characteristics that are similar to the disturbed sites in DCEW. Moreover, in the context of the previous studies noting the lag between aboveground and belowground C stocks, additional confirmation of this interpretation could arise through investigation of whether the amount of soil C observed contemporarily at the disturbed sites is consistent with the time since biomass removal.

4.3. Comparison and appropriateness of modeling approaches

Our primary study motivations were to: (1) understand the factors contributing to spatial variation in soil C in our semi-arid experimental watershed, (2) identify readily available landscape metrics that reflect these factors and (3) use these variables to develop models to predict soil C distribution across the landscape. In light of the objectives of this exploratory exercise, the two predictive modeling approaches used have similarities and differences that serve as useful guideposts for future studies.

Multiple linear regression is a widely used, simple approach to develop predictive models from soil C observations and extrapolate predictions to locations without observations, in this case based on the spatial distribution of a surrogate measure of vegetation productivity and potential insolation. The regression model building exercise indicates that aboveground vegetation density (represented in the model as NDVI) and insolation (represented in the model as potential insolation) are good predictors of the spatial variation of soil C and N. Given the simplicity of the model building approach and the widespread availability of topographic and vegetation data, a multiple

regression approach could more generally be applied to predict soil C distributions in semiarid regions at much broader scales. Unlike the cokriging approach, the linear regression method allows prediction where soil carbon data is not already available. As noted above, to better convey relative effects of predictor variables on soil C we constructed the regression models using standardized quantities for both predictor and response variables. As a result, the developed regression models require some estimate of the regional mean and variance in soil C to be used to predict the spatial distribution of soil C at broader scales. Predictive models developed using non-standardized quantities yield both similar structure and predictive power (not shown). However, developing algorithms to retrieve an estimate of soil C at similar resolutions and over large areas from remote sensing observations using a regression approach will require estimation of regional soil C statistics or the use of non-standardized predictor and response variables.

The cokriging approach is a slightly more complex method for developing predictive models, but is, nevertheless, a linear, variance-minimizing interpolation scheme. While the cokriging interpolation algorithm takes into consideration the covariates determined from the regression model building exercise, spatially distributed predictions are heavily weighted towards soil C observations. Moreover, in contrast to the regression approach, cokriging model development considers explicitly the spatial arrangement of observations in the development of predictive models. As a result, cokriging is better able to exploit spatial trends in the data itself to produce spatially distributed predictions of soil C. Another advantage of the cokriging approach is that it yields not only a spatially distributed prediction of soil C, but also a corresponding spatial distribution of prediction errors. Such a map is a particularly valuable asset for informing future soil C data collection.

4.4. Future modeling efforts

The statistical models used in this study to develop spatial predictions of soil C in DCEW may not sufficiently represent nonlinearities governing biogeochemical cycling – and the coupling of biogeochemical and hydrologic processes – in this semi-arid region. As such, future effort to develop spatial predictions of soil C will be directed toward the use of physically based, distributed ecosystem and ecohydrology models (e.g., Ivanov et al., 2008; Moorcroft et al., 2001; Running and Hunt, 1993). One particular strength of the soil carbon dataset developed in this study is as a constraint of physically based models in a data assimilation context. Data assimilation schemes, which combine uncertain model predictions with noisy observations, such as the ensemble Kalman Filter (EnKF) can leverage non-linear process models of biogeochemical cycling and be used to assimilate a broad suite of observations (Harmon and Challenor, 1997; Williams et al., 2005). Importantly, it has been previously demonstrated that inferences about nutrient cycling based on a modeling and data assimilation approach can be different from the conclusions reached using approaches using observations alone. Williams et al. (2005) provide a particularly illustrative example, using the EnKF to assimilate a broad diversity of observations into an ecosystem model to constrain net ecosystem carbon exchange and the partitioning of carbon into aboveground and belowground C pools. They concluded that the interior Oregon forest under study was a net atmospheric C sink; an approach relying on observations alone suggested the forest was a small net source. Data assimilation frameworks can yield both the temporal dynamics of C cycling and partitioning, as well as measures of predictive uncertainty.

4.5. Implications for soil carbon management and climate change

Interestingly, the models predict that nearly 44% of the total soil carbon (C) is found in the upper 1/3 of the watershed while the lower 1/3 of the watershed stores less than 19% of the watershed's soil C. In the middle third of the watershed modeling indicates most of the soil C storage (72%) is on the north-facing slopes. In the context of preserving existing soil C reservoirs, these observations suggest that the impact of disturbance (via climate or land use changes) on existing soil C stores will be highly spatially variable. Furthermore, given the close relationship with vegetative cover, soil C contents are likely to be sensitive to predicted temperature induced (i.e. Mote and Salathé, 2010) declines in vegetative cover.

5. Conclusions

The Dry Creek Experimental Watershed extends across a wide, elevation induced, precipitation and temperature range that produces steep gradients in above and below ground carbon (C) and nitrogen (N) pools. Even more dramatic variations in above and below ground C and N are observed with changes in aspect. Despite these large variations, a significant amount of the variance in the soil C distribution is explained by a combination of potential insolation and vegetation cover, as represented by NDVI. Both of these variables are easily calculated from widely available geospatial data, making this approach potentially useful for widespread application in complex, semi-arid landscapes. The use of these predictors to predict the distribution of soil C and N can facilitate better ecosystem management and rehabilitation practices at the local scale and improve understanding of the fate of soil C stores under the influence of a changing climate.

Acknowledgements

Funding provided by NSF-EPSCOR (EPS-0447689), Bureau of Land Management, and the U.S. Army RDECOM ARL Army Research Office under grant W911NF-09-1-0534. We wish to thank two anonymous reviewers whose insight and suggestions significantly improved our article.

References

Antos, J.A., Halpern, C.B., Miller, R.E., Cromack Jr., K., Halaj, M.G., 2003. Temporal and spatial changes in soil carbon and nitrogen after clearcutting and burning of an old-growth Douglas-fir forest. USDA Pacific Northwest Research Station. PNW-RP-552.
Arrouays, D., Daroussin, J., Kicin, J.L., Hassika, P., 1998. Improving topsoil carbon storage prediction using a digital elevation model in temperate forest soils of France. Soil Science Society of America Journal 163 (2), 103–108.
Arrouays, D., Saby, N., Walter, C., Lemercier, B., Schvartz, C., 2006. Relationships between particle-size distribution and organic carbon in French arable topsoils. Soil Use and Management 22 (1), 48–51.
Batjes, N.H., 1996. Total carbon and nitrogen in the soils of the world. European Journal of Soil Science 47, 151–163.
Beaudette, D.E., O'Geen, A.T., 2009. Quantifying the aspect effect: an application of solar radiation modeling for soil survey. Soil Science Society of America Journal 73, 1245–1352.
Burnham, J.H., Sletten, R.S., 2010. Spatial distribution of soil organic carbon in northwest Greenland and underestimates of high Arctic carbon stores. Global Biogeochemical 24, GB3012.
Burnham, W.L., Wood, S.H., 1992. Geologic map of the Boise South quadrangle, Ada County, Idaho, Idaho Geological Survey Technical Report Series, April 15, 1992.
Camarero, L., Garcia-Pausas, J., Huguet, C., 2009. A method for upscaling soil parameters for use in a dynamic modelling assessment of water quality in the Pyrenees. Science of the Total Environment 407 (5), 1701–1714.
Carrera, A.L., Mazzarino, M.J., Bertiller, M.B., del Valle, H.F., Carretero, E.M., 2009. Plant impacts on nitrogen and carbon cycling in the Monte Phytogeographical Province, Argentina. Journal of Arid Environments 72, 192–201.
Curran, P.J., Dungan, J.L., Gholz, H.L., 1992. Seasonal LAI in Slash Pine Estimated with Landsat TM. Remote Sensing of Environment 39, 3–13.
DCEW, 2010. Dry Creek Experimental Watershed. http://icewater.boisestate.edu/, accessed 1 May, 2010.
Delbari, M., Loiskandl, W., Afrasiab, P., 2010. Uncertainty assessment of soil organic carbon content spatial distribution using geostatistical stochastic simulation. Australian Journal of Soil Research 48 (1), 27–35.
Dingman, S.E., Koutz, F.R., 1974. Relations among vegetation, permafrost, and potential insolation in Central Alaska. Arctic and Alpine Research 6 (1), 37–42.
Don, A., Schumacher, J., Scherer-Lorenzen, M., Scholten, T., Schulze, E., 2007. Spatial and vertical variation of soil carbon at two grassland sites – implications for measuring soil carbon stocks. Geoderma 141, 272–282.

Florinsky, I.V., Eilers, R.G., Manning, G.R., Fuller, L.G., 2002. Prediction of soil properties by digital terrain modeling. Environmental Modelling and Software 17, 295–311.
Foley, J.A., Ramankutty, N., 2004. A primer on the Terrestrial Carbon Cycle. What We Don't Know But Should. 2004: The global carbon cycle: integrating humans, climate, and the natural world. In: Field, C.B., Raupach, M.R. (Eds.), The Global Carbon Cycle "SCOPE series", vol. 62. Island Press, Washington.
Franzmeier, D.P., Pederson, E.J., Longwell, T.J., Byrne, J.G., Losche, C.K., 1969. Properties of some soils of the Cumberland Plateau as related to slope aspect and position. Proceedings of the Soil Sciences Society of America. 33, 755–762.
Garcia-Pausas, J., Casals, P., Camarero, L., Huguet, C., Sebastiá, M., Thompson, R., Romanya, J., 2007. Soil organic carbon storage in mountain grasslands of the Pyrenees: effects of climate and topography. Biogeochemistry 82, 279–289.
Geroy, I.J., 2010. Factors influencing soil moisture at the hillslope scale in a semi-arid mountainous environment. MS thesis Boise State University.
Geroy I.J., Gribb, M.M., Marshall, H.P., Chandler, D.G., Benner, S.G., and McNamara, J.P., (In Review). Aspect influences on soil water retention and storage. Hydrological Processes.
Gribb, M.M., Forkutsa, I., Hansen, A., Chandler, D.G., McNamara, J.P., 2009. The effect of various soil hydraulic property estimates on soil moisture simulations. Vadose Zone Journal 8 (2), 321–331.
Harkness, A., 1997. Soil survey of Boise Front Project, Idaho. Interim and supplemental report. U.S. Dept. of Agriculture, Boise, Idaho.
Harmon, R., Challenor, P., 1997. A Markov chain Monte Carlo method for estimation and assimilation into models. Ecological Modeling 101 (1), 41–59.
Hooker, T.D., Stark, J.M., Norton, U., Leffler, A.J., Peek, M., Ryel, R., 2008. Distribution of ecosystem C and N within contrasting vegetation types in a semiarid rangeland in the Great Basin, USA. Biogeochemistry 90, 291–308.
Ivanov, V.Y., Bras, R.L., Vivoni, E.R., 2008. Vegetation-hydrology dynamics in complex terrain of semi-arid areas: 1. A mechanistic approach to modeling dynamic feedbacks. Water Resources Research 44.
Jensen, J.R., 2000. Remote sensing of the environment: an earth resource perspective. Upper Saddle River Prentice-Hall.
Jobbagy, E.G., Jackson, R.B., 2000. The vertical distribution of soil organic carbon and its relation to climate and vegetation. Ecological Applications 10 (2), 423–436.
Jordan, C.F., 1969. Derivation of leaf area index from quality measurements of light on the forest floor. Ecology 50, 663–666.
Kane, E.S., Valentine, D.W., Schuur, E.A.G., Dutta, K., 2005. Soil carbon stabilization along climate and stand productivity gradients in black spruce forests of interior Alaska. Canadian Journal of Forestry Research 35, 2118–2129.
Kriegler, F.J., Malila, W.A., Nalepka, R.F., Richardson, W., 1969. Preprocessing transformations and their effect on multispectral recognition. Proceedings of the sixth International Symposium on Remote Sensing of Environment. University of Michigan, Ann Arbor, MI, pp. 97–131.
Kulmatiski, A., Vogt, D.J., Siccama, T.G., Tilley, J.P., Kolesinskas, K., Wickwire, T.W., Larson, B.C., 2004. Landscape determinants of soil carbon and nitrogen storage in southern New England. Soil Science Society of America Journal 68 (6), 2014–2022.
Law, B.E., Thornton, P.E., Irvine, J., Anthoni, P.M., Van Tuyl, S., 2001. Carbon storage and fluxes in ponderosa pine forests at different developmental stages. Global Change Biology 7, 755–777.
Lee, R., 1964. Potential insolation as a topoclimatic characteristic of drainage basins. Hydrological Sciences Journal 9 (1), 27–41.
Lewis, R.S., Kiilsgaard, T.H., Bennett, E.H., Hall, W.H., 1987. Lithologic and chemical characteristics of the central and southeastern part of the southern lobe of the Idaho Batholith. In: Vallier, T.L., Brooks, H.C. (Eds.), Geology of the Blue Mountains region of Oregon, Idaho, and Washington – the Idaho Batholith and its border zone: U.S. Geologic Survey, Professional Paper, 1436, pp. 171–196.
Loutre, M.-F., Paillard, D., Vimeux, F., Cortijo, E., 2004. Does me\an annual insolation have the potential to change the climate? Earth and Planetary Science Letters 221, 1–14.
Majka, D., Jenness, J., Beier, P., 2007. CorridorDesigner: ArcGIS tools for designing and evaluating corridors. Available at http://corridordesign.org.
McClaran, M.P., Moore-Kucera, J., Martens, D.A., van Haren, J., Marsh, S.E., 2008. Soil carbon and nitrogen in relation to shrub size and death in a semi-arid grassland. Geoderma 145, 60–68.
Melillo, J.M., Borchers, J., Chaney, J., Fisher, H., Fox, S., Haxeltine, A., Janetos, A., Kicklighter, D.W., Kittel, T., Mcguire, A., Mckeown, R., Neilson, R., Nemani, R., Ojima, D., Painter, T., Pan, Y., Parton, W., Pierce, L., Pitelka, L., Prentice, C., Rizzo, B., Rosenbloom, N., Running, S., Schimel, D., Sitch, S., Smith, T., Woodward, I., 1995. Vegetation ecosystem modeling and analysis project – comparing biogeography and biogeochemistry models in a continental-scale study of terrestrial ecosystem responses to climate-change and CO_2 doubling. Global Biogeochemical Cycles 9 (4), 407–437.
Miller, J.O., Galbraith, J.M., Daniels, W.L., 2004. Soil organic carbon content in frigid southern Appalachian mountain soils. Soil Science of America Journal 68, 194–203.
Moorcroft, P.R., Hurtt, G.C., Pacala, S.W., 2001. A method for scaling vegetation dynamics: the ecosystem demography model. Ecological Monographs 71 (4), 557–585.
Mote, P.W., Salathé, E.P., 2010. Future Climate in the Pacific Northwest. Climatic Change 102, 29–50. doi:10.1007/s10584-010-9848-z.
Naoum, S., Tsanis, I.K., 2004. Orographic precipitation modeling with multiple linear regression. Journal of Hydrologic Engineering © ASCE 79–102 March/April.
Norton, J.B., Monaco, T.A., Norton, J.A., Johnson, D.A., Jones, T.A., 2004. Cheatgrass invasion alters soil morphology and organic matter dynamics in Big Sagebrush-Steppe rangelands. USDA Forest Service Proceedings RMRS-P-31, pp. 57–63.
NRCS, 2004. Soil Survey Laboratory Methods Manual, Soil Survey Investigations Report No. 42 Version 4.0.
NRCS, 2010. SNOTEL Data Collection Network Fact Sheet. http://www.wcc.nrcs.usda.gov/factpub/sntlfct1.html/, accessed 1 May, 2010.
Paruelo, J.M., Piñeiro, G., Baldi, G., Baeza, S., Lezama, F., Altesor, A., Oesterheld, M., 2010. Carbon stocks and fluxes in rangelands of the Río de la Plata Basin. Rangeland Ecology & Management 63 (1), 94–108.
Ranhao, S., Baiping, Z., Jing, T., 2004. A Multivariate regression model for predicting precipitation in the Daqing Mountains. Mountain Research and Development 28 (3/4), 318–325.
Reid, I., 1973. The influence of slope orientation upon the soil moisture regime, and its hydrogeomorphological significance. Journal of Hydrology 19, 309–321.
Rhoton, F.E., Emmerich, W.E., Goodrich, D.C., Miller, S.N., McChesney, D.S., 2006. Soil geomorphological characteristics of a semiarid watershed: influence on carbon distribution and transport. Soil Science of America Journal 70, 1532–1540.
Rodriguez-Iturbe, I., Porporato, A., Laio, F., Ridolfi, L., 2001. Plants in water-controlled ecosystems: active role in hydrologic processes and response to water stress – I. Scope and general outline. Advances in Water Resources 24 (7), 695–705.
Rouse, J.W., Hass, R.H., Schell, J.A., Deering, D.W., 1974. Monitoring vegetation systems in the Great Plains with ERTS. Proceedings, Third Earth Resources Technology Satellite-1 Symposium, Greenbelt.
Running, S.W., Hunt Jr., E.R., 1993. Generalization of a forest ecosystem process model for other biomes, BIOME-BGC, and an application for global-scale models. In: Ehleringer, J.R., Field, C. (Eds.), Scaling Processes Between Leaf and Landscape Levels. Academic Press, Orlando, pp. 141–158.
Scanlon, T.M., Albertson, J.D., Caylor, K.K., Williams, C.A., 2002. Determining land surface fractional cover from NDVI and rainfall time series for a savanna ecosystem. Remote Sensing of Environment 82, 376–388.
Shrestha, G., Stahl, P.D., 2008. Carbon accumulation and storage in semi-arid sagebrush steppe: effects of long-term grazing exclusion. Agriculture Ecosystems & Environment 125, 173–181.
Slesak, R.A., Schoenholtz, S.H., Harrington, T.B., Strahm, B.D., 2009. Dissolved carbon and nitrogen leaching following variable logging-debris retention and competing-vegetation control in Douglas-fir plantations of western Oregon and Washington. Canadian Journal of Forest Research 39, 1484–1497.
Smith, T.J., 2010. Using soil moisture trends across topographic gradients to examine controls on semi-arid ecosystem dynamics. MS thesis Boise State University.
Smith, T.J., McNamara, J.P., Flores, A.N., Gribb, M.M., Aishlin P.S., Benner, S.G., (In review). Limited soil storage capacity constrains upland benefits of winter snowpack. Hydrological Processes.
Tesfa, T.K., Tarboton, D.G., Chandler, D.G., McNamara, J.P., 2009. Modeling soil depth from topographic and land cover attributes. Water Resources Research 45, W10438.
Thompson, J.A., Kolka, R.K., 2005. Soil carbon storage estimation in a forested watershed using quantitative soil-landscape modeling. Soil Science Society of America Journal 69, 1086–1093.
Tsui, C.C., Chen, Z.S., Hsieh, C.F., 2004. Relationships between soil properties and slope position in a lowland rain forest of southern Taiwan. Geoderma 123, 131–142.
Vasques, G.M., Grunwald, S., Comerford, N.B., Sickman, J.O., 2010. Regional modelling of soil carbon at multiple depths within a subtropical watershed. Geoderma 156, 326–336.
Vedrova, E.F., Mukhortova, L.V., Ivanov, V.V., Krivobokov, L.V., Boloneva, M.V., 2010. Post-logging organic matter recovery in forest ecosystems of eastern Baikal region. Biology Bulletin 37 (1), 69–79.
Wang, L., Yi, C., Xu, X., Schutt, B., Liu, K., Zhou, L., 2009. Soil properties in two soil profiles from terraces of the Nam Co Lake in Tibet, China. Journal of Mountain Science 6, 354–361.
Webster, R., Oliver, M.A., 2007. Geostatistics for Environmental Scientists, second edition. John Wiley & Sons, The Atrium, Southern Gate, Chichester, West Sussex, England.
Webster, K.L., Creed, L.F., Beall, F.D., Bourbonniere, R.A., 2011. A topographic template for estimating soil pools in forested catchments. Geoderma 160, 457–467.
Williams, C.J., 2005. Characterization of the spatial and temporal controls on soil moisture and streamflow generation in a semi-arid headwater catchment. MS Thesis, Boise State University.
Williams, M., Schwarz, P.A., Law, B.E., Irvine, J., Kurpius, M.R., 2005. An improved analysis of forest carbon dynamics using data assimilation. Global Change Biology 11 (1), 89–105. doi:10.1111/j.1365-2486.2004.00891.x.
Yanai, R.D., Currie, W.S., Goodale, C.L., 2003. Soil carbon dynamics after forest harvest: an ecosystem paradigm reconsidered. Ecosystems 6, 197–212.
Yetemen, O., Istanbulluoglu, E., Vivoni, E.R., 2010. The implications of geology, soils, and vegetation on landscape morphology: inferences from semi-arid basins with complex vegetation patterns in Central New Mexico, USA. Geomorphology 116, 246–263.
Yimer, F., 2007. Soil Properties in Relation to Topographic Aspects, Vegetation Communities and Land Use in the South-eastern Highlands of Ethiopia. Doctoral thesis, Swedish University of Agricultural Sciences. Uppsala.
Zhusi, K., 2006. Spatial distribution of soil carbon and nitrogen storage and forest productivity in a watershed planted to Japanese cedar (Cryptomeria japonica D. Don). Journal of Forest Research 11, 351–358.